Crystal structure of a murine α-class glutathione *S*-transferase involved in cellular defense against oxidative stress

Ute Krengel[1,a], Klaus-Hasso Schröter[2,a], Helga Hoier[3,a], Anita Arkema[a], Kor H. Kalk[a], Piotr Zimniak[b], Bauke W. Dijkstra[a,*]

[a]*Laboratory of Biophysical Chemistry and BIOSON Research Institute, Department of Chemistry, University of Groningen, Nijenborgh 4, 9747 AG Groningen, Netherlands*

[b]*Departments of Medicine, and Biochemistry and Molecular Biology, University of Arkansas for Medical Sciences, Little Rock, AR 72205, USA*

Received 10 October 1997; revised version received 29 December 1997

Abstract Glutathione *S*-transferases (GSTs) are ubiquitous multifunctional enzymes which play a key role in cellular detoxification. The enzymes protect the cells against toxicants by conjugating them to glutathione. Recently, a novel subgroup of α-class GSTs has been identified with altered substrate specificity which is particularly important for cellular defense against oxidative stress. Here, we report the crystal structure of murine GSTA4-4, which is the first structure of a prototypical member of this subgroup. The structure was solved by molecular replacement and refined to 2.9 Å resolution. It resembles the structure of other members of the GST superfamily, but reveals a distinct substrate binding site.

Key words: Crystal structure; Glutathione; Glutathione *S*-transferase; Lipid peroxidation; Oxidative stress

1. Introduction

Glutathione *S*-transferases (GSTs; EC 2.5.1.18) catalyze the nucleophilic attack of the thiol group of glutathione on electrophilic groups of a wide variety of hydrophobic compounds, including environmental and industrial toxicants as well as drugs. The glutathione adducts produced by the reaction are often less toxic and generally have greater water solubility than the free compounds, which facilitates their removal from the cell. In this way, the enzymes contribute significantly to cellular detoxification, but likewise constitute an important factor in drug resistance of tumor cells during chemotherapy. In addition, GSTs are involved in intracellular storage and transport of hydrophobic non-substrate compounds including hormones, metabolites and drugs (see for reviews [1–7]).

Based on their sequence homology, substrate specificity and immunological cross-reactivity, GSTs have been grouped into five species-independent classes of isoenzymes. Four of these classes (α, π, μ and θ) comprise cytosolic enzymes, a fifth rather distinct form is microsomal [1,8–10]. All cytosolic GSTs are found to be homo- or hetero-dimeric enzymes (from within the same class) with a relative molecular mass of ca. 50 kDa [11]. The subunits are catalytically independent [12].

Over the past few years, crystal structures have been reported for all four classes of cytosolic GSTs [7,13–20]. The overall structures of these proteins are similar. They comprise an N-terminal αβ domain and a C-terminal all α-helical domain. In the active site, which is situated in spatially equivalent positions in the different classes, two distinct subsites are present: a glutathione binding site (G-site) and a pocket which accommodates the hydrophobic substrates (H-site). Recently, also structural results on microsomal GST have been obtained by electron diffraction [21].

A few years ago, a subgroup of α-class GSTs has been identified that acts primarily on endobiotic (endogenous) rather than on xenobiotic (exogenous) substrates [22–24]. In particular, electrophilic products of lipid peroxidation (e.g. 4-hydroxynonenal or fatty acid or phospholipid hydroperoxides) can be converted by this subclass of GSTs. These compounds are formed upon exposure of the cells to oxidative stress. Many of them are highly toxic and could contribute to the onset of severe diseases, such as atherosclerosis, which is the leading cause of death in Western industrialized countries. The above mentioned specialized forms of GST are able to limit the ensuing cellular damage in two ways: they reduce fatty acid hydroperoxides through their glutathione peroxidase activity, and they conjugate the already formed degradation products with glutathione. The detoxification activity of this subgroup of GSTs has been shown to be physiologically relevant, as demonstrated by transfection experiments [25–27].

Here, we report the crystal structure analysis of mGSTA4-4 (formerly named GST 5.7 with respect to its isoelectric point) and present for the first time the structure of a member of this subgroup of specialized GSTs.

2. Materials and methods

2.1. Purification and crystallization

Recombinant murine GSTA4-4 has been overexpressed in *Escherichia coli* and purified as described earlier [24]. For crystallization, the lyophilized protein was dissolved in water to a final concentration of 5–10 mg/ml. A broad range of conditions led to crystal formation. Best results were obtained at 20°C using the hanging-drop vapor diffusion method. 3 μl of the protein solution was mixed with equal amounts of the reservoir solution consisting of 9–12% PEG 8000, 5–10% MPD or 10 mM EDTA, and 0.1 M of one of the following

*Corresponding author. Fax: (31) (50) 363 4800.
E-mail: bauke@chem.rug.nl

[1]Present address: Department of Biochemistry and Biophysics, Chalmers University of Technology and Göteborg University, Lundberg Laboratory, 41390 Göteborg, Sweden.

[2]Present address: Astra Hässle AB, Preclinical IST, PS HET 252, 43183 Mölndal, Sweden.

[3]Present address: Institut für Kristallographie, Freie Universität Berlin, Takustr. 6, 14195 Berlin, Germany.

Abbreviations: GST, glutathione *S*-transferase; MPD, 2-methyl-2,4-pentanediol; r.s.c.c., real space correlation coefficient; r.m.s.d., root mean square difference

PII S0014-5793(98)00026-X

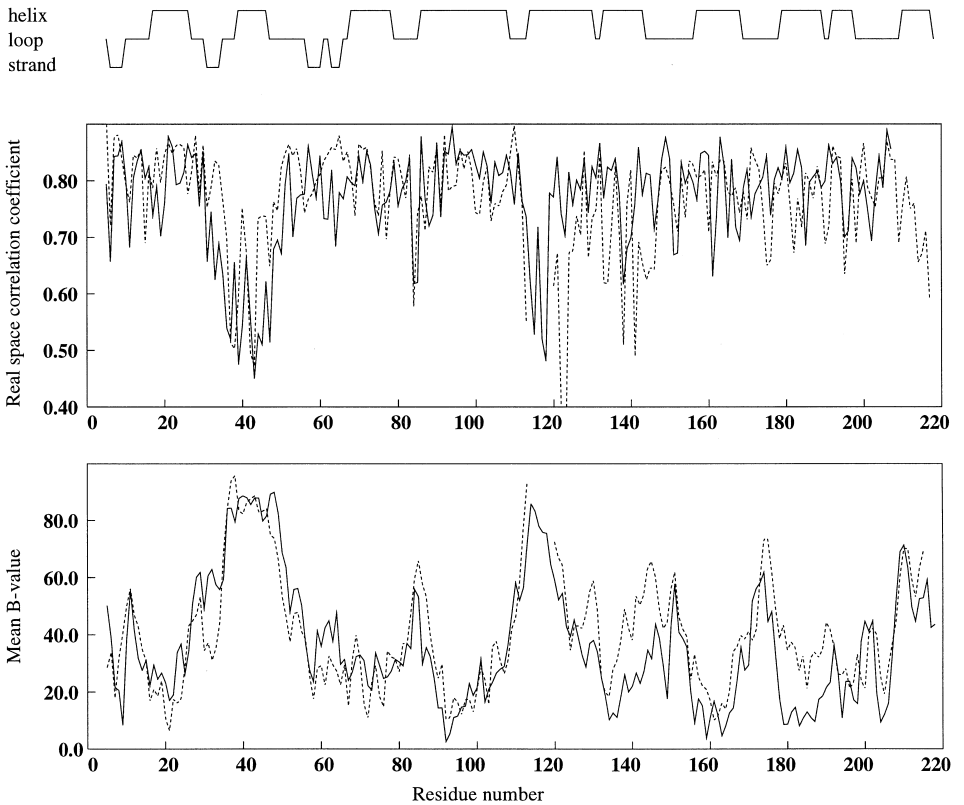

Fig. 1. Real space correlation coefficients for the σ_A-weighted (2Fo−Fc) OMIT map and mean *B*-values for molecule A (continuous line) and molecule B (dotted line) of the final model of mGSTA4-4, as a function of residue number. The majority of the differences occurring between the two monomers are caused by different crystal contacts. Note that residues 114–119 of molecule B were omitted from the final model, as these residues were found to be highly disordered in the crystal structure. The secondary structure is indicated in the top curve, shown as a 3-value function.

buffers: MES, pH 6.0 or HEPES, pH 7.0 or Tris-HCl, pH 8.0. After a few days, rod-shaped crystals appeared, which grew to a final size of ca. $0.4\times0.15\times0.15$ mm^3 within 2 weeks. The space group was determined to be $P2_12_12$, with cell dimensions of $a=114.3$ Å, $b=95.9$ Å and $c=50.8$ Å.

2.2. X-ray diffraction experiments

A 2.9 Å data set was collected at room temperature at the SRS, Daresbury Laboratory, at beam line 9.5 ($\lambda=1.04$ Å), which was equipped with a small MAR image plate. X-ray diffraction data were processed with DENZO and SCALEPACK [28], using a σ cutoff of 0. The data set is 80.1% complete (75.8% in the last resolution shell from 3.0 to 2.9 Å), comprising 10477 unique reflections with an average redundancy of 2.7. *R*sym(I) is 7.6% (31.9% in the last resolution shell) and the average I/σ value 8.8.

2.3. Molecular replacement

The crystal structure of murine GSTA4-4 was solved by molecular replacement, using the atomic coordinates of human GSTA1-1 [20] (accessible from the PDB under ID code 1GUH) as a search model. All calculations were carried out with the hGSTA1-1 dimer, using the Groningen BIOMOL package. The cross-rotation function showed a clear peak at $\alpha=133.8°$, $\beta=42.5°$, $\gamma=237.5°$, and the solution of the translation search was found to be $x=0.33$, $y=0.24$, $z=0.47$. The crystallographic *R*-factor for this solution was 40.8%, confirming also that the space group is $P2_12_12$ rather than $P2_12_12_1$.

2.4. Crystallographic refinement

The mGSTA4-4 crystal structure was refined with the program X-PLOR, version 3.843 [29], using the parameters of Engh and Huber [30]. As a starting model, the hGSTA1-1 coordinates were used, of which all non-conserved residues other than glycines were changed to alanine residues. During the first refinement cycles, simulated annealing techniques were applied, later on only conventional positional refinement was carried out. During the whole course of refinement, except for the final cycle, strong NCS restraints were applied. The progress during refinement was monitored by inspection of σ_A-weighted [31] (2Fo−Fc) OMIT maps [32,33]. Manual rebuilding was done with O [34]. In cases of doubt, the respective residues were omitted during a subsequent refinement cycle, keeping the neighboring residues fixed.

Refinement converged at an *R*-factor of 22.9% and a free *R*-factor (calculated from 10% of the reflections) of 30.3%. The last refinement cycle was repeated for all the reflections including the test set, resulting in a final *R*-factor of 23.4%. The final model comprises residues 5–219 of the 222 residues of molecule A and residues 5–113 and 120–217 of molecule B. Refinement statistics are summarized in Table 1. Coordinates have been submitted to the Protein Data Bank under accession code 1GUK.

3. Results and discussion

3.1. Quality of the final model

The three-dimensional structure of mGSTA4-4 was solved by molecular replacement using the coordinates of hGSTA1-1 [20] (Brookhaven Protein Data Bank code 1GUH) as a search model. The final 2.9 Å model comprises residues 5–219 of molecule A and residues 5–113 and 120–217 of molecule B. The N- and C-terminal ends of mGSTA4-4 as well as segment 114–119 of molecule B are highly disordered in the crystal structure. The corresponding helical segment in molecule A is somewhat better defined by electron density, as residues 115 and 119 of this molecule are involved in crystal contacts. However, as can be seen from Fig. 1, this region is one of the two most flexible parts of the protein structure.

Apart from the flexible regions of mGSTA4-4, the structure

is quite well defined by electron density, as is reflected by the average real space correlation coefficient (r.s.c.c.) for the final (2Fo−Fc) OMIT map of 0.77. The final crystallographic *R*-factor is 23.4%. Root mean square deviations from ideal geometry of 0.014 Å and 1.71° for bond lengths and angles, respectively, and the Ramachandran plot (Fig. 2) are consistent with a geometrically well defined structure. The one outlier which is present in the Ramachandran plot (Val-174 of molecule A) is well supported by its electron density (r.s.c.c. of OMIT map is 0.81).

3.2. Overall structure

Murine GSTA4-4 crystallizes in space group $P2_12_12$, containing one dimer per asymmetric unit. This dimer most likely corresponds to the fully functional mGSTA4-4 homodimer. The two GST subunits are related to one another by a non-crystallographic two-fold axis, creating a V-shaped interface typical for GSTs in general. The two GST monomers exhibit root mean square differences (r.m.s.d.) for C_α atoms of 0.11 Å, an artificially low value resulting from the use of NCS restraints during refinement (for comparison: the mean coordinate error as determined from a Luzzati plot [35] is ca. 0.4 Å). As the models for the different subunits are so similar and in view of the fact that our model of molecule B contains a gap of six missing amino acid residues (114–119), we will in the following focus on molecule A.

Fig. 3A gives a stereo view of the overall structure of the mGSTA4-4 monomer. It consists of two domains, an N-terminal αβ domain with βαβαββα topology and a C-terminal all α-helical domain which comprises helices α4–α9. The two domains are separated by a pronounced cleft which harbors the substrate (H-site) and glutathione (G-site) binding sites. The structure is very similar to that of human GSTA1-1, the only other α-class GST of which the structure is known to date. R.m.s. differences of C_α atoms are 0.78 Å for GST monomers. In particular, the two N-terminal domains superimpose very well with r.m.s. differences of 0.46 Å, while the C-terminal domains (r.m.s.d. = 0.85 Å compared to 1GUH) exhibit somewhat greater differences (shifts of 1–1.5 Å), concentrated in the upper half of domain 2 as represented in Fig. 3A. This region corresponds to the C-terminal part of helix α4, helix α5′ and connecting loop (residues 97–131) as well as to the loop region connecting helices α6 and α7 (residues 170–176). As residues 104–111 of helix α4 are implicated in substrate binding and residues 101 and 131 have been found to be important for binding glutathione [20], the observed differences, albeit small, might not be negligible.

3.3. Glutathione binding site

As murine GSTA4-4 has a rather high Michaelis constant (K_M = 0.5 mM [36], compared to a typical value of 0.1 mM for other GSTs [37]), it was expected that glutathione could be completely removed from the protein by extensive dialysis against water. However, inspection of the final (2Fo−Fc) map revealed density at positions corresponding to the binding site of glutathione in human GSTA1-1 (PDB entry 1GUH). Although glutathione is certainly not bound with 100% occupancy, it can be assumed that some glutathione is still present in the mGSTA4-4 structure even after dialysis against 0.1% acetic acid. Against our expectations, we are thus not dealing with the apo-form of the protein, but with the glutathione-bound form. However, the density of glutathione is rather weak, and we therefore did not include its coordinates in the final model of the mGSTA4-4 structure.

Considering that we are in fact dealing with the glutathione-bound form of mGSTA4-4 readily explains the existence of the C-terminal helix α9. For hGSTA1-1, this helix was found to be present in complexes with two different inhibitors and with its glutathione conjugate, but not in the unliganded form of the enzyme [20,38]. In analogy, we did not expect the C-terminal residues to adopt an α-helical conformation in the apo-form of mGSTA4-4.

A comparison of the glutathione binding site of mGSTA4-4 and hGSTA1-1 reveals two major differences: one of them concerns Arg-15 and the other one residues 41 and 45. Arg-15 is conserved in both α-class enzymes. In the hGSTA1-1 crystal structure, this residue interacts with the sulfur atom of glutathione [20]. It is fixed in this position by Glu-104, to which it forms a salt bridge. In mGSTAA4-4, Glu-104 is replaced by a methionine residue. Obviously, Met-104 cannot interact with Arg-15 in the same way as Glu-104. Instead, hydrophobic interactions are found to occur which involve the hydrophobic part of the arginine side chain (distance Met-104 C_ε to Arg-15 C_γ is 3.6 Å). Although the guanidinium part of the Arg-15 side chain can still adopt roughly the same conformation as in hGSTA1-1, this part of the residue is now much less fixed and develops *B*-factors of ca. 60 $Å^2$. For comparison, the Arg-15 guanidinium group of hGSTA1-1,

Table 1
Refinement statistics

Resolution range (Å)	10–2.9
Reflections used (Fo≥5)	9798
Final *R*-factor[a] (%)	23.4
Average real space correlation coefficient	
σ_A-weighted (2Fo−Fc) map	0.80
σ_A-weighted (2Fo−Fc) OMIT map	0.77
r.m.s. deviations from ideality for bond lengths (Å)	0.014
r.m.s. deviations from ideality for bond angles (°)	1.71
Number of non-H atoms (dimer)	3432
Average *B*-factors ($Å^2$)	40.6
Secondary structure analysis according to PROCHECK [41]	
Residues in most favored regions (%)	83.1
Residues in additional allowed regions (%)	14.8
Residues in generously allowed regions (%)	1.9
Residues in disallowed regions (%)	0.3
Protein Data Bank code	1GUK

[a] $R\text{-factor} = (\Sigma||Fo|-|Fc||/\Sigma|Fo|)$.

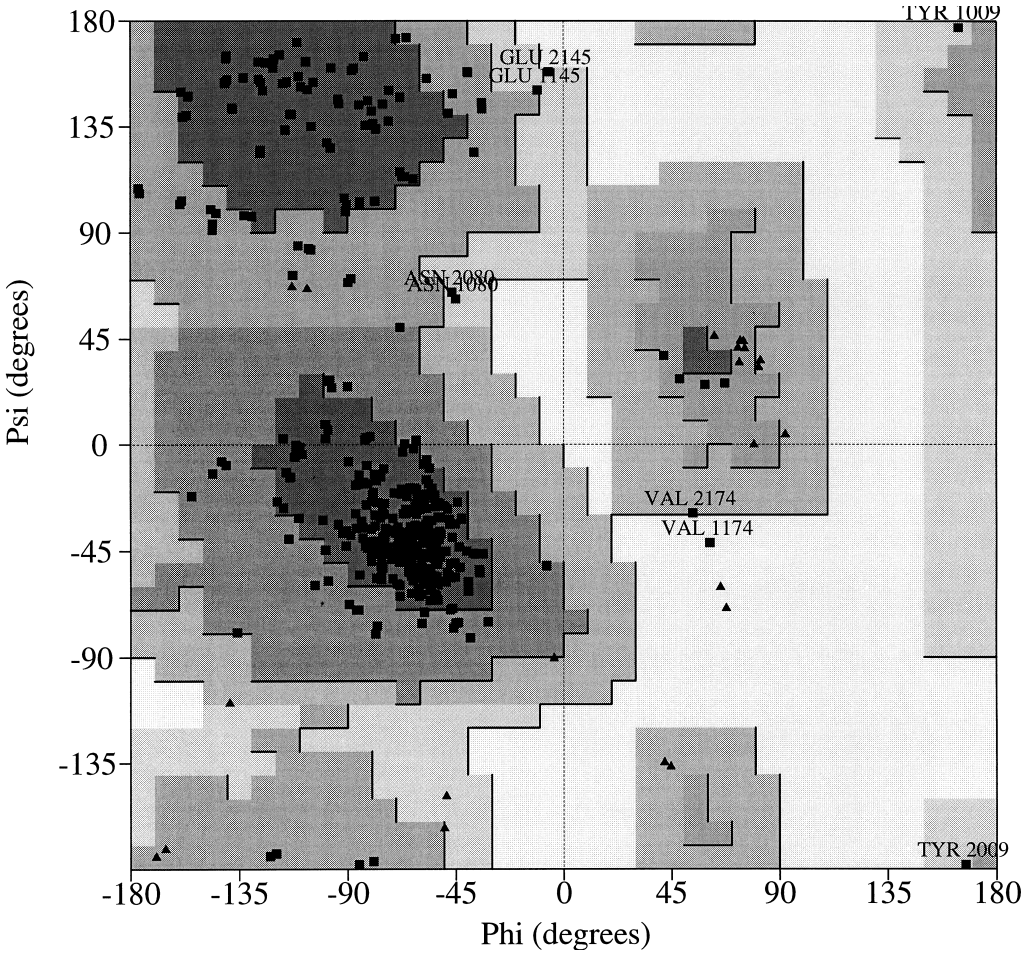

Fig. 2. Ramachandran plot as obtained from PROCHECK [41]. Val-174 of molecule A (named 1174) has unfavorable φ,ψ angles. However, its conformation is well supported by electron density (real space correlation coefficient of OMIT map is 0.81).

even in the apo-form of the enzyme (PDB entry 1GSD), only has temperature factors of about 25 $Å^2$.

The other major difference in the G-sites of mGSTA4-4 and hGSTA1-1 concerns residues 41 and 45. In hGSTA1-1, these residues are a leucine and an arginine, respectively, while they are replaced by a tyrosine and a glutamine residue in mGSTA4-4. Arg-45 has been found to interact with the glutathione carboxy-terminus in hGSTA1-1 [20]. Gln-45 of murine GSTA4-4 is much shorter and therefore cannot adopt the same function. Tyr-41, on the other hand, has a larger side chain than the respective Leu-41 of hGSTA1-1. In mGSTA4-4, this residue takes over the function of Arg-45 of hGSTA1-1. The tyrosine OH atom and the arginine NH_2 atom are basically superimposable. Tyr-41 is stabilized in this position by two hydrogen bonds involving the backbone carbonyl of residue 53 (2.9 Å) and the amide group of Gln-45 (3.1 Å). However, even if Tyr-41 adopts the most suitable conformation for binding glutathione, it cannot perform equally compared to Arg-45 of hGSTA1-1, as it cannot mimic the ionic interactions with the glutathione carboxy terminus.

Hence, the low binding constant of mGSTA4-4 for glutathione can be explained on the basis of its crystal structure and results from a combination of two structural differences, one involving the altered interaction of Arg-15 leading to enhanced flexibility of its guanidinium group, and the other one resulting from the incomplete substitution of function of Arg-45 by Tyr-41 of mGSTA4-4.

3.4. H-site

Murine GSTA4-4 and related enzymes are remarkable for two reasons: not only do they catalyze glutathione conjugation of endogenous substrates, in contrast to most GSTs which act on xenobiotics, but also their substrate specificity is reversed. As an example, both mGSTA4-4 and hGSTA1-1 have a similar activity for the model substrate 1-chloro-2,4-dinitrobenzene, but they differ by a factor of 100 in their activity towards 4-hydroxynonenal, a toxic electrophile derived from peroxidation products of unsaturated fatty acids [24,39,40].

The different specificity pattern of the two enzyme subclasses is expected to result from structural differences in the substrate binding site. For hGSTA1-1, this binding site has been described for three different inhibitor complexes, involving *S*-benzyl-glutathione (PDB entry 1GUH [20]), ethacrynic acid (1GSD [38]) and the glutathione conjugate of the latter compound (1GSF [38]). Three different regions were reported to be implicated in inhibitor binding, namely the N-terminus of helix α1, the C-terminus of helix α4 and the region immediately prior to and on one edge of helix α9.

For mGSTA4-4, the substrate binding site has been examined on the basis of a superposition of its crystal structure

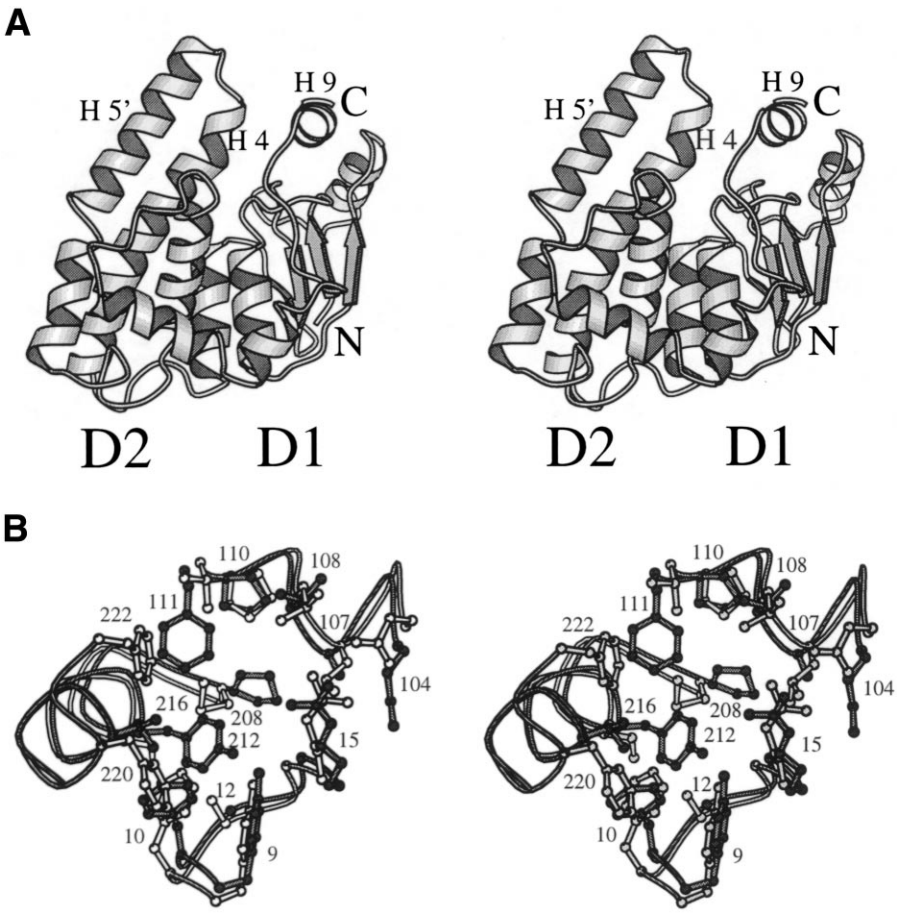

Fig. 3. A: Stereo view of the overall structure of one subunit of mGSTA4-4. Domain 1 and 2, the N- and C-terminus as well as helices 4, 5′ and 9 have been labelled. B: Stereo view of the substrate binding site of mGSTA4-4 (dark lines) compared to hGSTA1-1 (PDB ID code 1GUH) (light line). Both figures were prepared with Molscript [42].

with the structures of the three mentioned inhibitor complexes of hGSTA1-1. Although in general the same protein regions seem to be involved in substrate binding, significant differences also exist.

Following the protein chain from N- to C-terminus, the first difference is found to involve Phe-10. In its conformation in mGSTA4-4, a clash with Phe-220 of the hGSTA1-1 glutathione complex would be inevitable (see Fig. 3B). Phe-220 has been found to be important for inhibitor binding in hGSTA1-1, thus suggesting Phe-10 to be involved in inhibitor binding of mGSTA4-4. However, in the hGSTA1-1 apo-enzyme, Phe-10 adopts a similar conformation as in mGSTA4-4. The difference compared to the glutathione complex of hGSTA1-1 might therefore be due to the presence of the apo-form in the mGSTA4-4 crystal, rather than representing an important difference compared to hGSTA1-1.

The second difference involves residues 107 and 108 which are positioned at the hydrophobic end of the substrate binding site. In mGSTA4-4, these residues are an alanine and a valine, respectively, while in hGSTA1-1, the equivalent residues are leucines, thus residues with much longer side chains. As a consequence of the different primary structures, the H-site of mGSTA4-4 is significantly elongated compared to hGSTA1-1.

Adjacent to residues 107 and 108 at the C-terminal end of helix α4, Phe-111 is likely to play an equally important role for interaction with hydrophobic substrates. In hGSTA1-1, this residue is a valine. The much more bulky phenylalanine side chain in its current position is very close in space to the inhibitor ethacrynic acid and to Phe-222 of hGSTA1-1. Phe-222 is disordered in the mGSTA4-4 crystal structure. Thus, these two residues, Phe-111 of mGSTA4-4 and Phe-222 of hGSTA1-1, are likely to have similar but highly specialized functions regarding substrate binding of the two enzymes.

Another 'almost clash' with ethacrynic acid of the hGSTA1-1 complex 1GSF is observed for Tyr-212 of mGSTA4-4. In hGSTA1-1, this residue is a serine. The tyrosine side chain is positioned near Met-208 of hGSTA1-1, a residue replaced by a proline in mGSTA4-4. Like the functional mates Phe-111/Phe-222, Tyr-212 and Met-208 also seem to have exchanged their function for substrate binding. But other than the former pair of residues, Tyr-212 and Met-208 not only occupy somewhat different positions, but also have different chemical properties – tyrosine bearing a polar group and being much more bulky than methionine. The positioning of the Tyr-212 side chain is made possible by another difference in primary structure: the replacement of Ala-12 by glycine in mGSTA4-4.

The last residue which should be mentioned here is Val-216, which is substituted by an alanine residue in hGSTA1-1. This residue also serves to reduce the width of the substrate binding site.

Taken together, the major differences of the H-sites of mGSTA4-4 and hGSTA1-1 concern residues 107, 108, 111,

208, 212, 216, and 222. While Ala-107 and Val-108 of mGSTA4-4 serve to elongate the substrate binding site, Phe-111, Tyr-212, and Val-216 make it narrower. This is exactly what we would expect to happen, considering that substrates such as 4-hydroxynonenal are longer and slimmer compared to inhibitors like ethacrynic acid. Hence, although most of the residues implicated in substrate binding have very similar functions in hGSTA1-1 and mGSTA4-4 (e.g. Tyr-9 and Arg-15), the observed differences account for the high degree of specialization of the two enzyme subclasses.

Acknowledgements: This work was supported in part by NIH Grant ES07804 to P.Z., and Grant ERBCHBGCT930386 from the European Community to B.W.D.

References

[1] Mannervik, B. (1985) Adv. Enzymol. Relat. Areas Mol. Biol. 57, 357–417.
[2] Mannervik, B. and Danielson, U.H. (1988) CRC Crit. Rev. Biochem. Mol. Biol. 23, 283–337.
[3] Pickett, C.B. and Lu, A.Y.H. (1989) Annu. Rev. Biochem. 58, 743–764.
[4] Armstrong, R.N. (1991) Chem. Res. Toxicol. 4, 131–140.
[5] Tsuchida, S. and Sato, K. (1992) CRC Crit. Rev. Biochem. Mol. Biol. 27, 337–384.
[6] Dirr, H., Reinemer, P. and Huber, R. (1994) Eur. J. Biochem. 220, 645–661.
[7] Wilce, M.C.J. and Parker, M.W. (1994) Biochim. Biophys. Acta 1205, 1–18.
[8] Medh, R.D. and Awasthi, Y.C. (1990) Clin. Chem. Enzyme Commun. 3, 267–280.
[9] Medh, R.D., Saxena, M., Singhal, S.S., Ahmad, H. and Awasthi, Y.C. (1991) Biochem. J. 278, 793–799.
[10] Singhal, S.S., Saxena, M., Ahmad, H. and Awasthi, Y.C. (1992) Biochim. Biophys. Acta 1116, 137–146.
[11] Mannervik, B. and Jensson, H. (1982) J. Biol. Chem. 257, 9909–9912.
[12] Danielson, U.H. and Mannervik, B. (1985) Biochem. J. 231, 263–267.
[13] Reinemer, P., Dirr, H.W., Ladenstein, R., Schaeffer, J., Gallay, O. and Huber, R. (1991) EMBO J. 10, 1997–2005.
[14] Reinemer, P., Dirr, H.W., Ladenstein, R., Huber, R., Lo Bello, M., Federici, G. and Parker, M.W. (1992) J. Mol. Biol. 227, 214–226.
[15] Garcia-Sáez, I., Párraga, A., Phillips, M.F., Mantle, T.J. and Coll, M. (1994) J. Mol. Biol. 237, 298–314.
[16] Ji, X., Zhang, P., Armstrong, R.N. and Gilliland, G.L. (1992) Biochemistry 31, 10169–10184.
[17] Ji, X., Armstrong, R.N. and Gilliland, G.L. (1993) Biochemistry 32, 12949–12954.
[18] Ji, X.H., Johnson, W.W., Sesay, M.A., Dickert, L., Prasad, S.M., Ammon, H.L., Armstrong, R.N. and Gilliland, G.L. (1994) Biochemistry 33, 1043–1052.
[19] Raghunathan, S., Chandross, R.J., Kretsinger, R.H., Allison, T.J., Penington, C.J. and Rule, G.S. (1994) J. Mol. Biol. 238, 815–832.
[20] Sinning, I., Kleywegt, G.J., Cowan, S.W., Reinemer, P., Dirr, H.W., Huber, R., Gilliland, G.L., Armstrong, R.N., Ji, X., Board, P.G., Olin, B., Mannervik, B. and Jones, T.A. (1993) J. Mol. Biol. 232, 192–212.
[21] Hebert, H., Schmidt-Krey, I., Morgenstern, R., Murata, K., Hirai, T., Mitsuoka, K. and Fujiyoshi, Y. (1997) J. Mol. Biol. 271, 751–758.
[22] Esterbauer, H., Cheeseman, K.H., Dianzani, M.U., Poli, G. and Slater, T.F. (1982) Biochem. J. 208, 129–140.
[23] Jensson, H., Guthenberg, C., Ålin, P. and Mannervik, B. (1986) FEBS Lett. 203, 207–209.
[24] Singhal, S.S., Zimniak, P., Sharma, R., Srivastava, S.K., Awasthi, S. and Awasthi, Y.C. (1994) Biochim. Biophys. Acta 1204, 279–286.
[25] Awasthi, Y.C., Zimniak, P., Awasthi, S., Singhal, S.S., Srivastava, S.K., Piper, J.T., Chaubey, M., Petersen, D.R., He, N.-G., Sharma, R., Singh, S.V., Khan, M.F., Ansari, G.A.S. and Boor, P.J. (1996) in: Glutathione *S*-Transferases: Structure, Function and Clinical Implications (Vermeulen, N.P.E., Mulder, G.J., Nieuwenhuyse, H., Peters, W.H.M. and van Bladeren, P.J., Eds.), pp. 111–124, Taylor and Francis, London.
[26] He, N.G., Singhal, S.S., Srivastava, S.K., Zimniak, P., Awasthi, Y.C. and Awasthi, S. (1996) Arch. Biochem. Biophys. 333, 214–220.
[27] Zimniak, L., Awasthi, S., Srivastava, S.K. and Zimniak, P. (1997) Toxicol. Appl. Pharmacol. 143, 221–229.
[28] Otwinowski, Z. (1993) in: Data Collection and Processing (Sawyer, L., Isaacs, N. and Bailey, S., Eds.), pp. 56–63, SERC Daresbury Laboratory, Warrington.
[29] Brünger, A.T., Kuriyan, J. and Karplus, M. (1987) Science 235, 458–460.
[30] Engh, R.A. and Huber, R. (1991) Acta Crystallogr. A47, 392–400.
[31] Read, R.J. (1986) Acta Crystallogr. A42, 140–149.
[32] Bhat, T.N. (1988) J. Appl. Crystallogr. 21, 279–281.
[33] Vellieux, F.M.D. and Dijkstra, B.W. (1997) J. Appl. Crystallogr. 30, 396–399.
[34] Jones, T.A., Zou, J.-Y., Cowan, S.W. and Kjelgaard, M. (1991) Acta Crystallogr. A47, 110–119.
[35] Luzzati, V. (1952) Acta Crystallogr. 5, 802–810.
[36] Nanduri, B., Hayden, J.B., Awasthi, Y.C. and Zimniak, P. (1996) Arch. Biochem. Biophys. 335, 305–310.
[37] Ketterer, B. and Christodoulides, L.G. (1994) Adv. Pharmacol. 27, 37–69.
[38] Cameron, A.D., Sinning, I., L'Hermite, G., Olin, B., Board, P.G., Mannervik, B. and Jones, T.A. (1995) Structure 3, 717–727.
[39] Singhal, S.S., Zimniak, P., Awasthi, S., Piper, J.T., He, N.G., Teng, J.I., Petersen, D.R. and Awasthi, Y.C. (1994) Arch. Biochem. Biophys. 311, 242–250.
[40] Zimniak, P., Singhal, S.S., Srivastava, S.K., Awasthi, S., Sharma, R., Hayden, J.B. and Awasthi, Y.C. (1994) J. Biol. Chem. 269, 992–1000.
[41] Laskowski, R.A., MacArthur, M.W., Moss, D.S. and Thornton, J.M. (1993) J. Appl. Crystallogr. 26, 283–291.
[42] Kraulis, P.J. (1991) J. Appl. Crystallogr. 24, 946–950.